




Improving the sensitivity of Kerr quantum nondemolition measurement via squeezed light

Stepan Balybin ^{1,2,*}, Dariya Salykina ^{1,2} and Farid Ya. Khalili ^{2,†}

¹*Faculty of Physics, M. V. Lomonosov Moscow State University, Leninskie Gory 1, Moscow 119991, Russia*

²*Russian Quantum Center, Skolkovo IC, Bolshoy Bulvar 30, Moscow 121205, Russia*



(Received 15 August 2023; accepted 16 October 2023; published 13 November 2023)

In S. N. Balybin *et al.* [*Phys. Rev. A* **106**, 013720 (2022)] the scheme of quantum nondemolition measurement of optical quanta that uses a resonantly enhanced Kerr nonlinearity in optical microresonators was analyzed theoretically. It was shown that using modern high- Q microresonators, it is possible to achieve sensitivity several times better than the standard quantum limit. Here we propose and analyze in detail a significantly improved version of that scheme. We show that by using a squeezed quantum state of the probe beam and the antisqueezing (parametric amplification) of this beam at the output of the microresonator, it is possible to reduce the measurement imprecision by about one order of magnitude. The resulting sensitivity allows us to generate and verify multiphoton non-Gaussian quantum states of light, making the scheme considered here interesting for quantum information processing tasks.

DOI: [10.1103/PhysRevA.108.053708](https://doi.org/10.1103/PhysRevA.108.053708)

I. INTRODUCTION

An ideal quantum measurement described by von Neumann's reduction postulate [1] does not perturb the measured observable N . The sufficient condition for implementation of such a measurement is the commutativity of the operator \hat{N} with the Hamiltonian \hat{H} of the combined system "measured object + meter" [2,3]

$$[\hat{N}, \hat{H}] = 0, \quad (1)$$

where

$$\hat{H} = \hat{H}_S + \hat{H}_A + \hat{H}_I, \quad (2)$$

with \hat{H}_S and \hat{H}_A the Hamiltonians of the object and the meter, respectively, and \hat{H}_I the interaction Hamiltonian. In Ref. [4] the term quantum nondemolition (QND) measurement was coined for this type of measurement.

In many cases, a sequence of measurements of a variable $N(t)$ is required, instead of a single measurement. The typical example is detection of external force acting on the object. In this case the value of \hat{N} has to be preserved between the measurements, which leads to another (also sufficient) commutativity condition

$$[\hat{N}, \hat{H}_S] = 0. \quad (3)$$

The observables which satisfy both conditions (1) and (3) are known as QND observables.

It follows from Eqs. (1) and (3) that the interaction Hamiltonian has to commute with the measured observable:

$$[\hat{N}, \hat{H}_I] = 0. \quad (4)$$

In the particular case of the measurement of the electromagnetic energy or the number of quanta, this means that nonlinear interaction of the electromagnetic field with the meter has to be used. A semigedanken example of such a measurement based on the radiation pressure effect was considered in Ref. [5].

Later, a more practical scheme based on the cubic (Kerr) optical nonlinearity [6,7] was proposed. In this scheme, the signal optical mode interacts with another (probe) mode by means of the optical Kerr nonlinearity. As a result, the phase of the probe mode φ_p is changed depending on the photon number N_s in the signal mode [the cross phase modulation (XPM)]. The subsequent interferometric measurement of this phase allows one to retrieve the value of N_s with the precision depending on the initial uncertainty of φ_p (see Sec. IV of Ref. [8] for details). In the ideal lossless case, the photon numbers in both modes are preserved. However, due to the XPM effect, the phase of the signal mode is perturbed proportionally to the probe mode energy uncertainty, thus fulfilling the Heisenberg uncertainty relation.

The natural sensitivity threshold for the QND measurement of the number of quanta is the standard quantum limit (SQL)

$$\Delta N_{\text{SQL}} = \sqrt{N}, \quad (5)$$

where N is the mean number of the measured quanta. It corresponds to the best possible sensitivity of a linear nonabsorbing meter [3], for example, a phase-preserving linear amplifier [9]. Starting from the initial work in [10], many proof-of-principle experiments based on the XPM idea were done (see the review articles in [11–13]). The sensitivity exceeding the SQL was demonstrated in these experiments, but the ultimate goal of the single-photon accuracy was not reached due to the insufficient values of the optical nonlinearity in highly transparent optical media.

*sn.balybin@physics.msu.ru

†farit.khalili@gmail.com

Recent advantages in the fabrication of high- Q monolithic and integrated microresonators [14], which combine very low optical losses with a high concentration of optical energy, promise a way to overcome this problem. This possibility was analyzed in detail in Ref. [8]. It was shown that the sensitivity of the Kerr-nonlinearity-based QND measurement schemes is limited by the interplay of two undesirable effects: the optical losses and the self-phase modulation (SPM) of the probe mode, which perturbs the probe mode phase proportionally to the energy uncertainty of this mode.

It was shown in Ref. [15] that in the ideal lossless case, the SPM effect can be compensated using the measurement of the optimal quadrature of the output probe field instead of the phase one. However, in the presence of the optical losses, only partial compensation is possible, limiting the sensitivity by the value

$$(\Delta N_s)^2 = \frac{1}{\Gamma_X^2} \left(\frac{1}{4\eta N_p} + (1-\eta)N_p\Gamma_S^2 \right) \quad (6)$$

[see Eq. (32) of [8]]. Here ΔN_s is the measurement error, N_p is the photon number in the probe mode, Γ_X and Γ_S are the dimensionless factors of the cross and the self-phase modulation, respectively [see Eqs. (25) and (42)], and η is the quantum efficiency of the measurement channel. The second term here stems from the SPM. Due to this term, the optimal value of N_p exists, which provides the minimum of ΔN_s ,

$$(\Delta N_s)^2 = \frac{\Gamma_S}{\Gamma_X^2} \epsilon, \quad (7)$$

where

$$\epsilon = \sqrt{\frac{1-\eta}{\eta}} \quad (8)$$

is the normalized loss factor. It was shown in Ref. [8] that using the best microresonators available now, a sensitivity $\Delta N_s \sim 10^2-10^3$ could be achieved.

Equations (6) and (7) imply that the probe mode is prepared in the coherent quantum state. At the same time, it was shown by Caves [16] that the sensitivity of optical interferometric measurements can be improved without increasing the optical power by using the nonclassical squeezed states of light with a decreased uncertainty of the phase quadrature. Currently, this method is routinely used in the laser gravitational-wave detectors [17,18] (see the review in [19]).

However, it is known that the squeezed states are vulnerable to optical losses. In the same work [16], Caves proposed also to use an additional degenerate optical parametric amplifier (antisqueezer) at the output of the interferometer to reduce impact of the losses in the optical elements located after this amplifier, including the photodetectors inefficiency. Note that usually the output losses constitute the major part of the total loss budget in optical interferometers (however, this could be not the case in the multimode configurations, where the imperfect mode matching between the squeezer and antisqueezer could play a significant role). Recently, this method was demonstrated experimentally [20].

In the present work we show that the sensitivity of the QND measurement scheme, considered in Ref. [8], can be radically improved using these techniques. This paper is organized

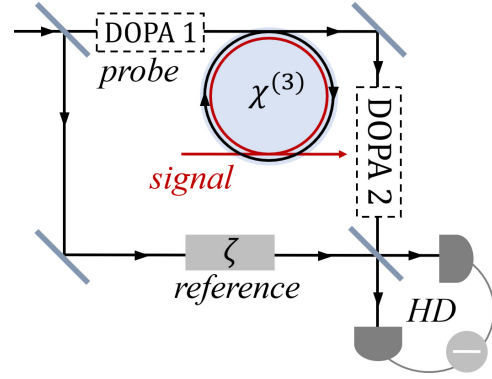


FIG. 1. Scheme of the QND measurement of the photon number in the signal mode via the XPM effect. Here DOPA denotes the degenerate optical parametric amplifier and HD the homodyne detector.

as follows. In Sec. II we derive the linearized input-output relations for the microresonator. In Sec. III we calculate the measurement error, taking into account the SPM effect and the losses in the probe mode. In Sec. IV we estimate the sensitivity, which can be achieved using the best available microresonators. In Sec. V we consider the effect of optical losses in the signal mode both in the measurement and in the quantum state preparation scenarios. In Sec. VI we discuss possible applications of the considered scheme to quantum information processing. We summarize the results of this paper in Sec. VII.

II. EVOLUTION OF OPTICAL FIELDS IN THE MICRORESONATOR

The measurement scheme is shown in Fig. 1. Here the strong coherent beam is split by the unbalanced beam splitter with transmissivity $T \ll 1$ into the probe and reference beams. The probe beam is squeezed by the first degenerate optical parametric amplifier (DOPA) 1 and then injected into the microresonator. There it interacts with the signal beam and then passes through DOPA 2 and finally is recombined with the reference beam in the homodyne detector.

Taking into account that the main goal of this paper is to show the advantages provided by the squeezing, and in order to simplify the calculations, we, similarly to Ref. [8], do not take into account explicitly the optical losses in the microresonator, but assume instead that

$$\frac{Q_{\text{load}}}{Q_{\text{intr}}} \approx \frac{\tau}{\tau^*} \ll \epsilon^2, \quad (9)$$

where Q_{load} is the loaded quality factor, Q_{intr} is the intrinsic one, τ is the interaction time, and τ^* is the relaxation time of the microresonator. In this case, the interaction of the signal and probe modes in the nonlinear microresonator can be described by the Hamiltonian [8]

$$\hat{H} = \sum_{j=p,s} \left(\hbar\omega_j \hat{N}_j - \frac{\hbar\gamma_S}{2} \hat{N}_j (\hat{N}_j - 1) \right) - \hbar\gamma_X \hat{N}_p \hat{N}_s, \quad (10)$$

where

$$\hat{N}_{p,s} = \hat{a}_{p,s}^\dagger \hat{a}_{p,s} \quad (11)$$

are the photon-number operators in the probe and signal modes, respectively, $\hat{a}_{p,s}$ and $\hat{a}_{p,s}^\dagger$ are the corresponding annihilation and creation operators for these modes, respectively, $\omega_{s,p}$ are their frequencies, and γ_S and γ_X are the coefficients of the SPM and XPM interactions, respectively. Evidently, both \hat{N}_p and \hat{N}_s commute with this Hamiltonian and therefore are preserved.

The corresponding Heisenberg equations of motion for the operators \hat{a}_s and \hat{a}_p are

$$\frac{d\hat{a}_p}{dt} = i(-\omega_p + \gamma_S\hat{N}_p + \gamma_X\hat{N}_s)\hat{a}_p, \quad (12a)$$

$$\frac{d\hat{a}_s}{dt} = i(-\omega_s + \gamma_S\hat{N}_s + \gamma_X\hat{N}_p)\hat{a}_s. \quad (12b)$$

The solution for the signal mode can be presented as

$$\hat{a}_s(t) = \exp[i(-\omega_s + \gamma_S\hat{N}_s + \gamma_X\hat{N}_p)t]\hat{a}_s, \quad (13)$$

which clearly shows that its phase is perturbed by (i) the XPM effect, which is the inevitable consequence of the uncertainty relation, and (ii) the parasitic SPM effect. A similar equation can be written for the probe mode. However, here we take into account that in order to implement the high-precision measurement, a large mean number of quanta in the probe mode N_p is required. This assumption allows us to linearize the probe mode equation of motion and thus smoothly integrate it into the general framework of the calculation of the optical interferometer.

We explicitly single out the part α_p in \hat{a}_p that contains the classical oscillation amplitude (that is, the average value of this operator):

$$\hat{a}_p \rightarrow \alpha_p + \hat{a}_p. \quad (14)$$

We suppose that classical amplitude is strong enough in comparison with the quantum one:

$$N_p = |\alpha_p|^2 \gg 1. \quad (15)$$

Without limiting the generality, we assume that α_p is real. In addition, we present the signal mode photon number as

$$\hat{N}_s + N_s + \delta\hat{N}_s, \quad (16)$$

where N_s is the mean value and $\delta\hat{N}_s$ is the *a priori* uncertainty, which we assume to be small:

$$\delta N_s \ll N_p. \quad (17)$$

Taking this into account, the classical part of Eq. (12a) can be presented as

$$\frac{d\alpha_p}{dt} = -i\omega'_p\alpha_p, \quad (18)$$

where

$$\omega'_p = \omega_p - \gamma_S\alpha_p^2 - \gamma_X N_s \quad (19)$$

is the dressed eigenfrequency of the probe mode. Subtracting Eq. (18) from Eq. (12a), keeping only terms of first order in \hat{a}_p and \hat{a}_p^\dagger , and using the rotated with frequency ω'_p picture, we obtain the linearized equation

$$\frac{d\hat{a}_p}{dt} = i\{N_p\gamma_S[\hat{a}_p(t) + \hat{a}_p^\dagger(t)] + \alpha_p\gamma_X\delta\hat{N}_s\}. \quad (20)$$

We introduce now cosine and sine quadratures of the pump mode:

$$\hat{a}_p^c = \frac{\hat{a}_p + \hat{a}_p^\dagger}{\sqrt{2}}, \quad \hat{a}_p^s = \frac{\hat{a}_p - \hat{a}_p^\dagger}{i\sqrt{2}}, \quad (21)$$

Using this notation, Eq. (20) can be rewritten as

$$\frac{d\hat{a}_p^c(t)}{dt} = 0, \quad (22a)$$

$$\frac{d\hat{a}_p^s(t)}{dt} = 2N_p\gamma_S\hat{a}_p^c(t) + \sqrt{2N_p}\gamma_X\delta\hat{N}_s. \quad (22b)$$

Integrating these equations, we obtain the input-output relations for the probe mode. In matrix notation, they can be presented as

$$\begin{pmatrix} \hat{b}_p^c \\ \hat{b}_p^s \end{pmatrix} \equiv \begin{pmatrix} \hat{a}_p^c(\tau) \\ \hat{a}_p^s(\tau) \end{pmatrix} = \mathbb{F} \begin{pmatrix} \hat{a}_p^c \\ \hat{a}_p^s \end{pmatrix} + \sqrt{2N_p}\Gamma_X\delta\hat{N}_s \begin{pmatrix} 0 \\ 1 \end{pmatrix}, \quad (23)$$

where

$$\mathbb{F} = \begin{pmatrix} 1 & 0 \\ 2N_p\Gamma_S & 1 \end{pmatrix} \quad (24)$$

is the SPM matrix, τ is the interaction time, and the factors $\Gamma_{X,S}$ are equal to

$$\Gamma_{X,S} = \gamma_{X,S}\tau. \quad (25)$$

III. SQUEEZING AND PARAMETRIC AMPLIFICATION

We assume that the probe field is prepared in the squeezed coherent state. In this case, using again the matrix notation, its initial state can be presented as

$$\begin{pmatrix} \hat{a}_p^c \\ \hat{a}_p^s \end{pmatrix} = \begin{pmatrix} \sqrt{2\alpha_p} \\ 0 \end{pmatrix} + \mathbb{S}(r, \theta) \begin{pmatrix} \hat{z}^c \\ \hat{z}^s \end{pmatrix}, \quad (26)$$

where the quadratures $\hat{z}^{c,s}$ correspond to a ground state field and

$$\mathbb{S}(r, \theta) = \begin{pmatrix} \cosh r + \sinh r \cos 2\theta & \sinh r \sin 2\theta \\ \sinh r \sin 2\theta & \cosh r - \sinh r \cos 2\theta \end{pmatrix} \quad (27)$$

is the squeeze matrix.

Transformation of the probe mode at the output of the microresonator by the second DOPA (the antisqueezer) can be described in a similar way,

$$\begin{pmatrix} \hat{c}_p^c \\ \hat{c}_p^s \end{pmatrix} = \mathbb{S}(R, \phi) \begin{pmatrix} \hat{b}_c \\ \hat{b}_s \end{pmatrix}, \quad (28)$$

where \hat{c}_p and \hat{c}_s describe the probe field at the output of DOPA 2 and R and ϕ are the corresponding squeeze factor and squeeze angle, respectively.

The resulting optical topology can be viewed as a non-linear single-arm SU(1, 1) interferometer (a more detailed discussion of interferometer types can be found in [19,21–23]). It is important to note that here we use an unbalanced configuration with $r \neq R$ and $\theta \neq \phi$.

The final step is the homodyne measurement of the quadrature

$$\hat{c}_p^\zeta = \mathbf{H}^\top(\zeta) \begin{pmatrix} \hat{c}_p^c \\ \hat{c}_p^s \end{pmatrix}, \quad (29)$$

defined by the homodyne angle ζ , where

$$\mathbf{H}(\zeta) = \begin{pmatrix} \cos \zeta \\ \sin \zeta \end{pmatrix} \quad (30)$$

is the homodyne vector. We take into account the output losses, including the detection inefficiency, by using the model of the imaginary beam splitter with the power transmissivity η , located before the detector (see [24]). It transforms the output signal as

$$\hat{d}_p^\zeta = \sqrt{\eta} \hat{c}_p^\zeta + \sqrt{1-\eta} \hat{y}, \quad (31)$$

where \hat{y} is the corresponding quadrature amplitude of a vacuum field.

Combining Eqs. (23), (28), and (31) and separating the signal term proportional to $\delta \hat{N}_s$ from other (noise) terms, we obtain the equation for the output signal

$$\hat{d}_p^\zeta = \hat{d}_0^\zeta + G \delta \hat{N}_s, \quad (32)$$

where

$$\hat{d}_0^\zeta = \sqrt{\eta} \mathbf{H}^\top(\zeta) \mathbb{S}(R, \phi) \mathbb{F} \begin{pmatrix} \hat{a}_c \\ \hat{a}_s \end{pmatrix} + \sqrt{1-\eta} \hat{y} \quad (33)$$

is the part of \hat{d}_p^ζ which does not depend on $\delta \hat{N}_s$ and

$$G = \sqrt{2\eta N_p} \Gamma_X \mathbf{H}^\top(\zeta) \mathbb{S}(R, \phi) \begin{pmatrix} 0 \\ 1 \end{pmatrix} \quad (34)$$

is the gain factor.

Therefore, the measurement error for the signal mode photon number is equal to

$$(\Delta N_s)^2 = \frac{(\Delta \hat{d}_0^\zeta)^2}{G^2}, \quad (35)$$

where $(\Delta \hat{d}_0^\zeta)^2$ is the variance of \hat{d}_0^ζ . It depends on three parameters: the squeeze angles θ and ϕ and the homodyne angle ζ , which have to be optimized. This optimization is done in the Appendix, giving the result

$$(\Delta N_s)_{\text{meas}}^2 = \frac{1}{\Gamma_X^2} \left(\frac{e^{-2r} + \epsilon^2 e^{-2R}}{4N_p} + \frac{N_p \Gamma_S^2 \epsilon^2}{e^{2R} + \epsilon^2 e^{2r}} \right). \quad (36)$$

A comparison of Eqs. (36) and (6) clearly shows that both the squeezing of the input probe field and the antisqueezing of the output one suppress the influence of the SPM, improving the sensitivity. Consider the structure of this equation in detail. In the lossless case ($\epsilon = 0$) it reduces to

$$(\Delta N_s)_{\text{meas}}^2 = \frac{1}{\Gamma_X^2} \frac{e^{-2r}}{4N_p}, \quad (37)$$

which is consistent with the results of Caves' paper [16] and shows the improvement of the sensitivity by the factor e^{-2r} beating the SQL limit. Note that, in this case, the antisqueezer does not affect the sensitivity. Taking into account the losses,

but without the SPM, we arrive at the formula

$$(\Delta N_s)_{\text{meas}}^2 = \frac{1}{\Gamma_X^2} \frac{e^{-2r} + \epsilon^2 e^{-2R}}{4N_p}. \quad (38)$$

One can see that the part which corresponds to losses is suppressed by a multiplier e^{-2R} (compare again with [16]). Finally, the last term in Eq. (36), which arises due to the SPM effect, also is suppressed by the antisqueezer.

The best possible sensitivity corresponds to the mean number of the probe photons equal to

$$N_p = \frac{e^{R-r} + \epsilon^2 e^{r-R}}{2\Gamma_S \epsilon}. \quad (39)$$

In this case,

$$(\Delta N_s)_{\text{meas}}^2 = \frac{\Gamma_S}{\Gamma_X^2} \epsilon e^{-r-R} \quad (40)$$

[compare with Eq. (7)].

In the practical case of $r \sim R$ and $\epsilon \ll 1$, N_p is proportional to e^R . However, as it was shown in Ref. [8], the typical values of the pump power are modest, on the order of microwatts. Therefore, N_p can be safely increased by a few orders of magnitude.

IV. SENSITIVITY ESTIMATES

For the numerical estimates, we use mostly the same parameters as in Ref. [8]. We consider a microresonator made of CaF₂, which has one of the highest intrinsic Q factors $Q_{\text{intr}} \simeq 3 \times 10^{11}$ [25]. In order to satisfy the requirement (9), we assume that

$$Q_{\text{load}} = 10^{10}. \quad (41)$$

We assume also that the optical wavelength in vacuum is $\lambda \approx 1.55 \mu\text{m}$ and the microresonator diameter is approximately equal to $100 \mu\text{m}$. In this case, the factors Γ_X and Γ_S can be estimated as

$$\Gamma_X = 2\Gamma_S = 2Q_{\text{load}} \frac{n_2 \hbar \omega_0 c}{n_0 V_{\text{eff}}} \approx 0.85 \times 10^{-5}, \quad (42)$$

where c is the speed of light, ω_0 is the optical frequency, n_0 is the refractive index of the material, n_2 is the cubic nonlinearity coefficient, V_{eff} is the effective volume of the mode, and $Q_{\text{load}} = \omega_0 \tau$ is the loaded quality factor. For the output losses, we use the moderately optimistic value $\eta \approx 0.9$.

Considering the squeezing, it should be taken into account that during the past decade, significant progress in this area has been achieved, stimulated in part by the requirements of laser gravitational-wave detectors. Values of squeezing exceeding 10 dB ($e^{-2r} = 0.1$) were demonstrated (see, e.g., Refs. [26,27]). Therefore, we use 10 dB for our estimates here.

It is worth noting that these values are limited mostly by the optical losses in the DOPAs. In the case of the antisqueezing, the results are affected by the losses to a much lesser degree. Therefore, here we explore higher values of the antisqueezing factor, up to 40 dB ($e^{2R} = 10^4$). Note that the values of the optical parametric gain exceeding 40 dB were already demonstrated experimentally (see, e.g., [28]).

In Fig. 2 the measurement error ΔN_s is plotted as a function of the photon number in the probe mode N_p for four scenarios:

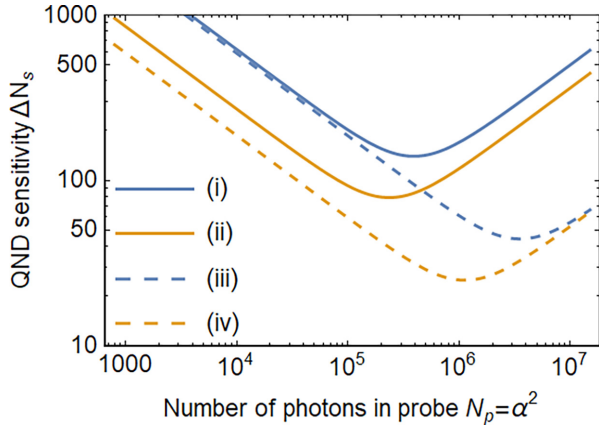


FIG. 2. Plot of the measurement error ΔN_s [see Eq. (36)] as a function of the photon number in the probe mode N_p for the four characteristic combinations of the squeezing and parametric amplification factors: (i) $r = R = 0$, (ii) $e^{-2r} = 0.1$ and $R = 0$, (iii) $r = 0$ and $e^{-2R} = 0.01$, and (iv) $e^{-2r} = 0.1$ and $e^{-2R} = 0.01$. In all cases, $\eta = 0.9$ and $\Gamma_X = 2\Gamma_S = 0.85 \times 10^{-5}$.

(i) without squeezing and parametric amplification, (ii) with squeezing and without parametric amplification, (iii) without squeezing and with amplification, and (iv) with squeezing and amplification. It can be seen from these plots that combining both these techniques, it is possible to reduce the measurement error by almost one order of magnitude, down to a few tens of photons.

The minima of these plots correspond to the optimal photon numbers in the probe mode, given by Eq. (39). In Fig. 3 the corresponding optimal values of the measurement error ΔN_s are plotted as functions of the parametric amplification factor e^{2R} , expressed for convenience in decibels. It can be seen from these plots that the sensitivity, corresponding to the preparation of the signal mode in a non-Gaussian state (see

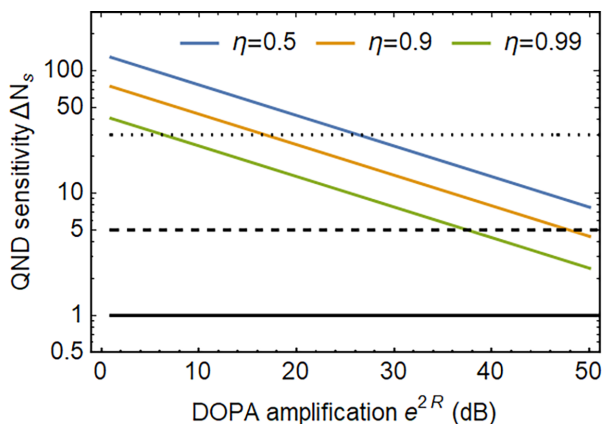


FIG. 3. Plot of the optimized measurement error ΔN_s [see Eq. (40)] as a function of the parametric amplification factor e^{2R} . In all cases, $e^{-2r} = 0.1$ (10 dB), $\eta = 0.9$, and $\Gamma_X = 2\Gamma_S = 0.85 \times 10^{-5}$. The black solid line corresponds to the single-photon sensitivity, the black dashed line corresponds to the five-photon sensitivity, and the black dotted line $\Delta N_s = 30$ approximately corresponds to the non-Gaussianity limit for $\mu \sim 0.01$ and $N_s \sim 10^3$ – 10^4 (see Sec. VI).

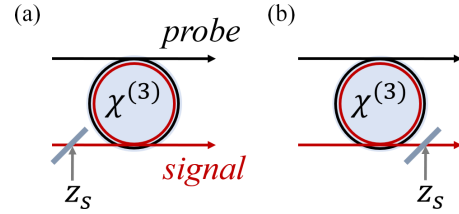


FIG. 4. Accounting for losses in the signal mode: (a) measurement of the incident number of quanta and (b) preparation of the output quantum state. In both cases, μ is the power transmissivity factor for the signal mode.

Sec. VI), could be achieved for reasonably optimistic values of the parametric amplification of the probe mode.

V. LOSSES IN THE SIGNAL MODE

In the previous sections we have taken into account the optical losses inside the microresonator (by mean of limiting the interaction time τ) and the output losses in the probe mode. Two other mechanisms of degrading the sensitivity are the input and output losses in the signal mode. The first one is relevant for the task of measuring the incident number of quanta and the second one for preparation of the output quantum state.

These two scenarios are shown in Fig. 4. In both cases, we model the losses by means of an imaginary beam splitter with power transmissivity μ , located either in the input or in the output path of the signal beam, respectively.

Let us start with the first case [see Fig. 4(a)]. In this case, the imaginary beam splitter transforms the input field as

$$\hat{a}_s = \sqrt{\mu}\hat{a}_{s\text{in}} + \sqrt{1-\mu}\hat{z}_s, \quad (43)$$

where the annihilation operator $\hat{a}_{s\text{in}}$ describes the incident field before the losses and \hat{z}_s corresponds to a ground-state field. Using this equation, it is easy to obtain the following relations for the mean numbers and the variances of the incident photon number $\hat{N}_{s\text{in}} = \hat{a}_{s\text{in}}^\dagger \hat{a}_{s\text{in}}$ and the intracavity one $\hat{N}_s = \hat{a}_s^\dagger \hat{a}_s$:

$$N_s = \mu N_{s\text{in}}, \quad (44a)$$

$$(\Delta N_s)^2 = \mu^2 (\Delta N_{s\text{in}})^2 + \mu(1-\mu)N_{s\text{in}}. \quad (44b)$$

The factor μ in Eq. (44a) decreases the gain factor (34): $G_{\text{loss}} = \mu G$. The second term in Eq. (44b) creates an additional uncertainty in the intracavity photon number and therefore has to be added to the measurement error (36). As a result, we obtain the following equation for the modified measurement error:

$$(\Delta N_s)_{\text{meas loss}}^2 = \frac{1}{\mu^2} [\mu(1-\mu)N_s + (\Delta N_s)_{\text{meas}}^2]. \quad (45)$$

It is instructive to normalize it by the initial mean number of photons:

$$\frac{(\Delta N_s)_{\text{meas loss}}^2}{N_s} = \frac{1-\mu}{\mu} + \frac{(\Delta N_s)_{\text{meas}}^2}{\mu^2 N_s}. \quad (46)$$

It is easy to see that the necessary condition for overcoming the SQL (5) is the inequality $\mu > \frac{1}{2}$, which corresponds to

the well-known limitation on losses in optical schemes using nonclassical states of light [29].

Consider now the second task, namely, the quantum state preparation [see Fig. 4(b)]. In this case, the mean value and the variance of the output photon number are equal to

$$N_{s\text{prep}} = \mu N_s, \quad (47a)$$

$$(\Delta N_s)_{\text{prep}}^2 = \mu^2 (\Delta N_s)_{\text{meas}}^2 + \mu(1-\mu)N_s \quad (47b)$$

[compare with Eqs. (44)]. We assumed here that the uncertainty of the intracavity number of quanta is equal to the measurement error $(\Delta N_s)_{\text{meas}}$. Normalizing this value by the mean number of the output photons (47a), we obtain

$$\frac{(\Delta N_s)_{\text{prep}}^2}{N_{s\text{prep}}} = 1 - \mu \left(1 - \frac{(\Delta N_s)_{\text{meas}}^2}{N_s} \right). \quad (48)$$

It is easy to see that in the case of the sub-SQL intracavity sensitivity, $(\Delta N_s)_{\text{meas}} < \sqrt{N_s}$, the prepared quantum state also will be a sub-Poissonian one, $(\Delta N_s)_{\text{prep}} < \sqrt{N_{s\text{out}}}$, for any value of μ .

VI. APPLICATIONS TO QUANTUM COMPUTING

We have shown that modern optical microresonators allow us to overcome the SQL (5). Another more demanding threshold is important for the continuous-variable quantum information processing applications [30]. It corresponds to the performance allowing us to generate and verify quantum states characterized by non-Gaussian negative-value Wigner quasiprobability distributions (non-Gaussian quantum states). Note that the Gaussian states cannot be orthogonal to each other [31], while orthogonality is necessary for many quantum phenomena. In particular, non-Gaussian states are required for quantum computation protocols that cannot be efficiently simulated by classical computers [32].

It is known [33,34] that the pure quantum states with the photon-number uncertainty satisfying the inequality (in this section we omit for brevity all numerical factors of order of unity)

$$\Delta N \lesssim N^{1/3}, \quad (49)$$

where N is the mean photon number, are non-Gaussian ones. Taking into account the losses in the signal mode [see Eqs. (44b) and (47b)] and assuming that $1 - \mu \ll 1$, this inequality leads to the requirement

$$(\Delta N_s)_{\text{meas}}^2 \lesssim N_s^{2/3} - (1 - \mu)N_s. \quad (50)$$

The maximum of the right-hand side of this condition is achieved at

$$N_s \sim \frac{1}{(1 - \mu)^3}, \quad (51)$$

giving the requirement

$$(\Delta N_s)_{\text{meas}} \lesssim \frac{1}{1 - \mu}. \quad (52)$$

For the reasonably optimistic values of $1 - \mu \sim 0.01$, this corresponds to the measurement imprecision of tens of photons. According to our estimates in Sec. IV (see Fig. 3), this value can be considered as a feasible one.

The next important threshold is the single-photon QND sensitivity, which will allow us to prepare and detect without absorption Fock states with an arbitrary number of quanta. It follows from Eqs. (44b) and (47b) that in the case of $(\Delta N_s)_{\text{meas}} \lesssim 1$ it can be reached with values of $N_s \sim 10$. The characteristics of modern microcavities, together with the experimentally achievable parameters of single-mode squeezing and antisqueezing, already make it possible to achieve a sensitivity of several photons (see the black dashed line in Fig. 4). Therefore, taking into account the contemporary rapid progress in both the fabrication of high- Q microresonators and the optical squeezing, it is possible to hope that the single-photon sensitivity will be implemented in a predictable future.

VII. CONCLUSION

We analyzed theoretically the application of squeezed states of light to the scheme considered in Ref. [8] of quantum nondemolition measurement of optical energy, based on the effect of cross-phase modulation in a microresonator. We showed that the sensitivity of this scheme can be radically improved using the squeezed quantum state of the probe beam and the antisqueezing (parametric amplification) of this beam at the output of the microresonator.

We considered the sensitivity limitations imposed by optical losses in both probe and signal modes and found the optimal values of the both squeeze angles minimizing the interfering effect of self-phase modulation. We showed that for reasonably optimistic values of the optical losses in the scheme, the squeezing allows us to improve the sensitivity of the QND measurement by about one order of magnitude, from a few hundreds of photons to a few tens.

Our estimates showed that this sensitivity allows us to generate and verify non-Gaussian quantum states, characterized by negative-value Wigner quasiprobability distributions. Therefore, the QND measurement scheme considered here could be interesting for quantum information processing tasks.

ACKNOWLEDGMENTS

This work was supported by the Russian Science Foundation (Project No. 20-12-00344). The work of S.B. was also supported by the Foundation for the Advancement of Theoretical Physics and Mathematics BASIS. The research of Sec. VI was supported by Rosatom within the framework of the Roadmap for Quantum Computing (Contracts No. 868-1.3-15/15-2021 and No. P2154).

APPENDIX: OPTIMIZATION OF THE SQUEEZE AND HOMODYNE ANGLES

Note that

$$\mathbf{H}^\top \mathbb{S}(R, \phi) = (CS), \quad (A1)$$

where

$$C = e^R \cos(\zeta - \phi) \cos \phi - e^{-R} \sin(\zeta - \phi) \sin \phi, \quad (A2a)$$

$$S = e^R \cos(\zeta - \phi) \sin \phi + e^{-R} \sin(\zeta - \phi) \cos \phi. \quad (A2b)$$

Therefore, it follows from Eqs. (34) and (33) that

$$G = \sqrt{2\eta N_p \Gamma_X S}, \quad (\text{A3})$$

$$\hat{d}_0^\zeta = \sqrt{\eta} (B\hat{a}_p^c + A\hat{a}_p^s) + \sqrt{1-\eta}\hat{y}, \quad (\text{A4})$$

where

$$A = S, \quad B = C + 2N_p \Gamma_S S. \quad (\text{A5})$$

The variances of the ground field quadratures $z^{c,s}$, \hat{y} , are equal to $\frac{1}{2}$. Therefore, taking into account Eq. (26), the variances of the quadratures $a_p^{c,s}$ and their covariance are equal to

$$\langle (\Delta\hat{a}_p^c)^2 \rangle = \frac{1}{2}(\cosh 2r + \sinh 2r \cos 2\theta), \quad (\text{A6a})$$

$$\langle (\Delta\hat{a}_p^s)^2 \rangle = \frac{1}{2}(\cosh 2r - \sinh 2r \cos 2\theta), \quad (\text{A6b})$$

$$\langle \hat{b}_p^c \circ \hat{b}_p^s \rangle = \frac{1}{2} \sinh 2r \sin 2\theta, \quad (\text{A6c})$$

where \circ denotes the symmetrized product and the variance of \hat{d}_0^ζ is equal to

$$\langle (\Delta\hat{d}_0^\zeta)^2 \rangle = \frac{\eta}{2} \{ (A^2 + B^2) \cosh 2r + [(-A^2 + B^2) \cos 2\theta + 2AB \sin 2\theta] \sinh 2r + \epsilon^2 \}. \quad (\text{A7})$$

The minimum of this equation in θ is provided by

$$\cos 2\theta = \frac{A^2 - B^2}{A^2 + B^2}, \quad \sin 2\theta = -\frac{2AB}{A^2 + B^2}. \quad (\text{A8})$$

Taking into account that G does not depend on θ , it corresponds also to the minimum of (35), equal to

$$\langle (\Delta N_s)^2 \rangle = \frac{(A^2 + B^2)e^{-2r} + \epsilon^2}{4N_p \Gamma_X^2 S^2}. \quad (\text{A9})$$

The next step is the optimization of this equation in ζ . In order to simplify the equations, we use the following approach. We assume first that the second squeezing is strong enough to

allow the following approximation:

$$\cosh 2R \approx \sinh 2R \approx \frac{e^R}{2}. \quad (\text{A10})$$

Note that this approximation holds very well even for moderate values of R . In this case,

$$C \approx e^R \cos(\zeta - \phi) \cos \phi, \quad S \approx e^R \cos(\zeta - \phi) \sin \phi, \quad (\text{A11})$$

and

$$\langle (\Delta N_s)^2 \rangle = \frac{1}{4N_p \Gamma_X^2 \sin^2 \phi} \left((1 + 2N_p \Gamma_S \sin 2\phi + 4N_p^2 \Gamma_S^2 \sin^2 \phi) e^{-2r} + \frac{\epsilon^2 e^{-2R}}{\cos^2(\zeta - \phi)} \right). \quad (\text{A12})$$

Evidently, the minimum of this equation is provided by

$$\zeta = \phi. \quad (\text{A13})$$

Note that for this value of ζ , C and S are given by the following exact equations:

$$C = e^R \cos \phi, \quad S = e^R \sin \phi. \quad (\text{A14})$$

Therefore, the following equation corresponds to also exact, albeit possibly not strictly minimal, value of the measurement error:

$$\langle (\Delta N_s)^2 \rangle = \frac{1}{4N_p \Gamma_X^2} \left[(1 + \cot^2 \phi + 4N_p \Gamma_S \cot \phi + 4N_p^2 \Gamma_S^2) e^{-2r} + \epsilon^2 (1 + \cot^2 \phi) e^{-2R} \right]. \quad (\text{A15})$$

The final step is the optimization in ϕ , which is straightforward:

$$\cot \phi = -\frac{2N_p \Gamma_S}{1 + \epsilon^2 e^{2r-2R}}. \quad (\text{A16})$$

As a result, we obtain Eq. (36).

-
- [1] J. von Neumann, *Mathematical Foundations of Quantum Mechanics: New Edition* (Princeton University Press, Princeton, 2018).
- [2] D. Bohm, *Quantum Theory* (Dover, Mineola, 1951).
- [3] V. B. Braginsky and F. Y. Khalili, *Quantum Measurement* (Cambridge University Press, Cambridge, 1992).
- [4] K. S. Thorne, R. W. P. Drever, C. M. Caves, M. Zimmermann, and V. D. Sandberg, Quantum nondemolition measurements of harmonic oscillators, *Phys. Rev. Lett.* **40**, 667 (1978).
- [5] V. B. Braginsky, Y. I. Vorontsov, and F. Y. Khalili, Quantum features of the ponderomotive meter of electromagnetic energy, *Sov. Phys. JETP* **46**, 705 (1977).
- [6] V. B. Braginsky and S. P. Vyatchanin, Nondestructive measurement of the energy of optical quanta, *Sov. Phys. Dokl.* **26**, 686 (1981).
- [7] G. J. Milburn and D. F. Walls, Quantum nondemolition measurements via quadratic coupling, *Phys. Rev. A* **28**, 2065 (1983).
- [8] S. N. Balybin, A. B. Matsko, F. Y. Khalili, D. V. Strekalov, V. S. Ilchenko, A. A. Savchenkov, N. M. Lebedev, and I. A. Bilenko, Quantum nondemolition measurements of photon number in monolithic microcavities, *Phys. Rev. A* **106**, 013720 (2022).
- [9] H. Heffner, The fundamental noise limit of linear amplifiers, *Proc. IRE* **50**, 1604 (1962).
- [10] M. D. Levenson, R. M. Shelby, M. Reid, and D. F. Walls, Quantum nondemolition detection of optical quadrature amplitudes, *Phys. Rev. Lett.* **57**, 2473 (1986).
- [11] J. F. Roch, G. Roger, P. Grangier, J.-M. Courty, and S. Reynaud, Quantum non-demolition measurements in optics: A review and some recent experimental results, *Appl. Phys. B* **55**, 291 (1992).
- [12] V. B. Braginsky and F. Y. Khalili, Quantum nondemolition measurements: The route from toys to tools, *Rev. Mod. Phys.* **68**, 1 (1996).
- [13] P. Grangier, J. A. Levenson, and J.-P. Poizat, Quantum non-demolition measurements in optics, *Nature (London)* **396**, 537 (1998).
- [14] D. V. Strekalov, C. Marquardt, A. B. Matsko, H. G. L. Schwefel, and G. Leuchs, Nonlinear and quantum optics with whispering gallery resonators, *J. Opt.* **18**, 123002 (2016).
- [15] P. D. Drummond, J. Breslin, and R. M. Shelby, Quantum-nondemolition measurements with coherent soliton probes, *Phys. Rev. Lett.* **73**, 2837 (1994).
- [16] C. M. Caves, Quantum-mechanical noise in an interferometer, *Phys. Rev. D* **23**, 1693 (1981).

- [17] M. Tse *et al.*, Quantum-enhanced advanced LIGO detectors in the era of gravitational-wave astronomy, *Phys. Rev. Lett.* **123**, 231107 (2019).
- [18] F. Acernese *et al.* (Virgo Collaboration), Increasing the astrophysical reach of the advanced virgo detector via the application of squeezed vacuum states of light, *Phys. Rev. Lett.* **123**, 231108 (2019).
- [19] D. Salykina and F. Khalili, Sensitivity of quantum-enhanced interferometers, *Symmetry* **15**, 774 (2023).
- [20] G. Frascella, S. Agne, F. Y. Khalili, and M. V. Chekhova, Overcoming detection loss and noise in squeezing-based optical sensing, *npj Quantum Inf.* **7**, 72 (2021).
- [21] B. Yurke, S. L. McCall, and J. R. Klauder, SU(2) and SU(1,1) interferometers, *Phys. Rev. A* **33**, 4033 (1986).
- [22] M. V. Chekhova and Z. Y. Ou, Nonlinear interferometers in quantum optics, *Adv. Opt. Photon.* **8**, 104 (2016).
- [23] K.-H. Luo, M. Santandrea, M. Stefszky, J. Sperling, M. Massaro, A. Ferreri, P. R. Sharapova, H. Herrmann, and C. Silberhorn, Quantum optical coherence: From linear to nonlinear interferometers, *Phys. Rev. A* **104**, 043707 (2021).
- [24] U. Leonhardt and H. Paul, Realistic optical homodyne measurements and quasiprobability distributions, *Phys. Rev. A* **48**, 4598 (1993).
- [25] A. A. Savchenkov, A. B. Matsko, V. S. Ilchenko, and L. Maleki, Optical resonators with ten million finesse, *Opt. Express* **15**, 6768 (2007).
- [26] H. Vahlbruch, M. Mehmet, K. Danzmann, and R. Schnabel, Detection of 15 dB squeezed states of light and their application for the absolute calibration of photoelectric quantum efficiency, *Phys. Rev. Lett.* **117**, 110801 (2016).
- [27] M. Mehmet and H. Vahlbruch, High-efficiency squeezed light generation for gravitational wave detectors, *Class. Quantum Grav.* **36**, 015014 (2019).
- [28] K. J. A. Ooi, D. K. T. Ng, T. Wang, A. K. L. Chee, S. K. Ng, Q. Wang, L. K. Ang, A. M. Agarwal, L. C. Kimerling, and D. T. H. Tan, Pushing the limits of CMOS optical parametric amplifiers with USRN : Si₇N₃ above the two-photon absorption edge, *Nat. Commun.* **8**, 13878 (2017).
- [29] R. Demkowicz-Dobrzański, K. Banaszek, and R. Schnabel, Fundamental quantum interferometry bound for the squeezed-light-enhanced gravitational wave detector GEO 600, *Phys. Rev. A* **88**, 041802(R) (2013).
- [30] S. L. Braunstein and P. van Loock, Quantum information with continuous variables, *Rev. Mod. Phys.* **77**, 513 (2005).
- [31] W. Schleich, *Quantum Optics in Phase Space* (Wiley-VCH, Berlin, 2001).
- [32] A. Mari and J. Eisert, Positive Wigner functions render classical simulation of quantum computation efficient, *Phys. Rev. Lett.* **109**, 230503 (2012).
- [33] R. S. Bondurant and J. H. Shapiro, Squeezed states in phase-sensing interferometers, *Phys. Rev. D* **30**, 2548 (1984).
- [34] M. Kitagawa and Y. Yamamoto, Number-phase minimum-uncertainty state with reduced number uncertainty in a Kerr nonlinear interferometer, *Phys. Rev. A* **34**, 3974 (1986).